Cellular/Molecular

Calcium Binding by Synaptotagmin's C_2A Domain is an Essential Element of the Electrostatic Switch That Triggers Synchronous Synaptic Transmission

Amelia R. Striegel,[1]* Laurie M. Biela,[1]* Chantell S. Evans,[2] Zhao Wang,[2] Jillian B. Delehoy,[1] R. Bryan Sutton,[3] Edwin R. Chapman,[2] and Noreen E. Reist[1]

[1]Department of Biomedical Sciences, Program in Molecular, Cellular, and Integrative Neuroscience, Colorado State University, Fort Collins, Colorado, 80523, [2]Department of Neuroscience, University of Wisconsin, Madison, Wisconsin, 53706, and [3]Department of Cell Physiology and Molecular Biophysics, Texas Tech University Health Sciences Center, Lubbock, Texas, 79409

Synaptotagmin is the major calcium sensor for fast synaptic transmission that requires the synchronous fusion of synaptic vesicles. Synaptotagmin contains two calcium-binding domains: C_2A and C_2B. Mutation of a positively charged residue (R233Q in rat) showed that Ca^{2+}-dependent interactions between the C_2A domain and membranes play a role in the electrostatic switch that initiates fusion. Surprisingly, aspartate-to-asparagine mutations in C_2A that inhibit Ca^{2+} binding support efficient synaptic transmission, suggesting that Ca^{2+} binding by C_2A is not required for triggering synchronous fusion. Based on a structural analysis, we generated a novel mutation of a single Ca^{2+}-binding residue in C_2A (D229E in *Drosophila*) that inhibited Ca^{2+} binding but maintained the negative charge of the pocket. This C_2A aspartate-to-glutamate mutation resulted in ~80% decrease in synchronous transmitter release and a decrease in the apparent Ca^{2+} affinity of release. Previous aspartate-to-asparagine mutations in C_2A partially mimicked Ca^{2+} binding by decreasing the negative charge of the pocket. We now show that the major function of Ca^{2+} binding to C_2A is to neutralize the negative charge of the pocket, thereby unleashing the fusion-stimulating activity of synaptotagmin. Our results demonstrate that Ca^{2+} binding by C_2A is a critical component of the electrostatic switch that triggers synchronous fusion. Thus, Ca^{2+} binding by C_2B is necessary and sufficient to regulate the precise timing required for coupling vesicle fusion to Ca^{2+} influx, but Ca^{2+} binding by both C_2 domains is required to flip the electrostatic switch that triggers efficient synchronous synaptic transmission.

Introduction

Synaptic transmission occurs when Ca^{2+} entry into an active nerve terminal triggers the fast, synchronous fusion of synaptic vesicles with the presynaptic membrane. Shortly after the identification of its two C_2 domains, synaptotagmin was postulated to be the Ca^{2+} sensor that triggers this synchronous fusion of vesicles (Brose et al., 1992). Initial studies suggested that the vesicle proximal C_2 domain, C_2A, mediated the Ca^{2+} binding that triggered synchronous vesicle fusion events (Elferink et al., 1993; Fernández-Chacón et al., 2001). However, mutations that inhibited Ca^{2+} binding by C_2A supported efficient synaptic transmission at excitatory synapses (Fernández-Chacón et al., 2002; Robinson et al., 2002; Stevens and Sullivan, 2003; Yoshihara et al., 2010). Mutations in the second C_2 domain, C_2B, that inhibited Ca^{2+} binding abolished evoked-transmitter release, demonstrating that Ca^{2+} binding by C_2B is essential for synchronous, Ca^{2+}-triggered transmitter release (Mackler et al., 2002). Thus, Ca^{2+} binding by the C_2B domain has been thought to be both necessary and sufficient for triggering synchronous transmitter release. Yet mutations that disrupted Ca^{2+}-dependent interactions by the C_2A domain decrease synchronous release by 50% and decrease the apparent Ca^{2+} affinity of release (Fernández-Chacón et al., 2001; Wang et al., 2003; Paddock et al., 2008, 2011), suggesting that Ca^{2+} binding by C_2A is required for efficient synchronous release. These results raised a now long-standing question: how can Ca^{2+}-dependent interactions by C_2A be functionally more significant than C_2A Ca^{2+} binding itself?

When synaptotagmin binds calcium, it alters the electrostatic potential of the calcium-binding pocket (Ubach et al., 1998), enhancing interactions with other presynaptic molecules, such as negatively charged membranes and proteins of the SNARE complex (Brose et al., 1992; Chapman et al., 1995; Schiavo et al., 1997; Chapman and Davis, 1998; Bai et al., 2002; Zhang et al., 2002). This suggests that both C_2 domains function as an electrostatic switch (Davletov et al., 1998; Ubach et al., 1998; Murray and Honig, 2002) such that the bound calcium ions shield, or effectively neutralize, the negative potential of the pocket. Such neu-

Received Sept. 11, 2011; revised Nov. 13, 2011; accepted Nov. 28, 2011.

Author contributions: E.R.C. and N.E.R. designed research; A.R.S., L.M.B., C.S.E., Z.W., and R.B.S. performed research; A.R.S., L.M.B., C.S.E., Z.W., J.B.D., R.B.S., and N.E.R. analyzed data; A.R.S., C.S.E., and N.E.R. wrote the paper.

This work was supported by grants from the National Institutes of Health (NS-045865 to N.E.R., MN-61876 to E.R.C.), the National Science Foundation (IOS-9982862 and IOS-1025966 to N.E.R.), the Microscope Imaging Network, and the College Research Council of Colorado State University. We thank Drs. Gary Pickard and Mike Tamkun for fruitful discussions and Dr. Deborah M. Garrity for comments on this manuscript.

E.R.C. is an Investigator of the Howard Hughes Medical Institute.

*A.R.S. and L.M.B. contributed equally to this paper.

Correspondence should be addressed to Dr. Noreen E. Reist, Department of Biomedical Sciences, Colorado State University, Fort Collins, CO 80523. E-mail: Noreen.Reist@Colostate.edu.

DOI:10.1523/JNEUROSCI.4652-11.2012

 0270-6474/12/321253-08$15.00/0

tralization permits residues at the tip of both the C_2A and C_2B Ca^{2+}-binding pockets, known to interact with negatively charged phospholipids (Chae et al., 1998; Fernández-Chacón et al., 2001; Bai et al., 2002; Wang et al., 2003), to interact with the presynaptic membrane. Thus, the previously tested aspartate-to-asparagine mutations (D→N) in C_2A, which inhibited Ca^{2+} binding by removing this negative charge, may result in minimal disruptions of synchronous transmitter release, or even enhance release, because the mutations partially mimic Ca^{2+} binding (Stevens and Sullivan, 2003).

Here we directly test the importance of electrostatic repulsion by C_2A in inhibiting fusion. We designed an aspartate-to-glutamate mutation (D→E) to test the function of Ca^{2+} binding independent of charge neutralization. This mutation inhibited Ca^{2+} binding but maintained the negative charge (and hence the repulsive force) of the C_2A Ca^{2+}-binding pocket. Our novel mutation, which cannot mimic the charge-neutralizing function of Ca^{2+} binding, results in a severe decrease in synchronous synaptic transmission, demonstrating that Ca^{2+} binding by C_2A is required for the electrostatic switch.

Materials and Methods

Mutagenesis. Drosophila synaptotagmin aspartate residue 229 was mutated to glutamate. Oligonucleotides (cttggtctcgaacttcttcttcttgtcgggcagc aagtacaccttgacatagggctccgaggtac and ctcggagccctatgtcaaggtgtacttgctgccc gacaagaagaagaagttcgagac) were used to create a mutant double-stranded DNA fragment with KpnI and StyI overhangs, which was ligated into a wild-type synaptotagmin cDNA construct in pBluescript II KS (Stratagene), sequenced, and subcloned into a pUAST vector to place the mutant *syt* gene under the control of the UAS promoter (Brand and Perrimon, 1993); then these were sent to Best Gene to transform *Drosophila*.

Fly lines. Expression of the transgene was localized to the nervous system using elavGAL4 to drive pan neuronal expression of the UAS-*syt* transgenes (Brand and Perrimon, 1993; Yao and White, 1994). The syt^{null} mutation used was syt^{AD4} (DiAntonio et al., 1993). Standard genetic techniques were used to cross the transgenes into the syt^{null} background to express the transgene in the absence of endogenous synaptotagmin 1 (Loewen et al., 2006a). No gender selection was used, thus a mix of male and female larvae were used in all experiments. Experimental flies were *yw;* syt^{null}*elavGAL4/*syt^{null}*; P[UAS* $syt^{A\text{-}D229E}$*]/+* ($P[syt^{A\text{-}D2E}]$, transgenic mutant) and *yw;* syt^{null}*elavGAL4/*syt^{null}*; P[UAS* syt^{WT}*]/+* ($P[syt^{WT}]$, transgenic control).

Sequence alignments. A ClustalW2 sequence alignment was performed on the C_2A domain of the following Ca^{2+}-binding synaptotagmin isoforms: syt 1 from *Drosophila melanogaster* (NP_523460.2), *Apis mellifera* (NP_001139207.1), *Manduca sexta* (AAK01129.1), *Loligo pealei* (BAA09866.1), *Caenorhabditis elegans* (NP_495394.3), *Gallus gallus* (NP_990502.1), *Mus musculus* (NP_033332.1), and *Rattus norvegicus* (NP_001028852.2); and *Homo sapiens* syt 1 (NP_001129277.1), syt 2 (NP_001129976.1), syt 3 (NP_001153801.1), syt 5 (NP_003171.2), syt 6 (NP_995320.1), syt 7 (NP_004191.2), syt 9 (NP_445776.1), and syt 10 (NP_945343.1).

Molecular modeling. The D2E mutation in Figure 1*C* was modeled using the mutagenesis plugin in PyMOL (The PyMOL Molecular Graphics System, Version 1.3; Schrödinger). Asp-178, from the high-resolution rat synaptotagmin 1 C_2A x-ray structure (Protein Data Bank, PDB file; 1RSY), was changed to a glutamate. The rotamer with the fewest number of collisions was selected for the figure.

Electrophysiology. Excitatory junction potentials (EJPs) and miniature EJPs (mEJPs) were recorded using standard techniques (Reist et al., 1998; Paddock et al., 2011) from L3 muscle fiber 6 of abdominal segments 3 and 4 in HL3 saline containing 70 mM NaCl, 5 mM KCl, 20 mM $MgCl_2$, 10 mM $NaHCO_3$, 5 mM Trehalose, 115 mM sucrose, 5 mM HEPES, pH 7.2, and 1.5 mM $CaCl_2$, unless otherwise indicated. Dissections were performed in Ca^{2+}-free HL3 saline. Fibers were impaled with a 10–40 MΩ recording electrode containing three parts 2 M potassium citrate to one part 3 M potassium chloride. The resting membrane potential of each fiber was maintained at −55 mV by passing a bias current. To evoke EJPs, segmental nerves were stimulated with a suction electrode filled with 1.5 mM Ca^{2+} HL3. The Ca^{2+} dependence curve was generated by averaging 10 EJPs recorded at 0.5 Hz from fibers bathed in HL3 containing Ca^{2+} concentrations ranging from 0.6 to 5.0 mM. Recordings in multiple Ca^{2+} concentrations were made from each muscle fiber. With the exception of 1.5 mM Ca^{2+}, 10–13 fibers were recorded at each Ca^{2+} concentration in each genotype. At 1.5 mM Ca^{2+}, 28–34 fibers were recorded, since most recording sessions included this concentration. All events were collected using an AxoClamp 2B (Molecular Devices) and digitized using a MacLab4s A/D converter (ADInstruments). The Ca^{2+}-dependence data were fit with the Hill equation using Kaleidagraph software. The Ca^{2+} cooperativity coefficient was estimated from the slope of a double-log plot of EJP amplitude versus Ca^{2+} concentration. EJPs were recorded in Scope software and mEJPs were recorded in Chart Software (ADInstruments).

Immunoblotting and immunohistochemistry. Western analysis was used to determine levels of transgene expression. The CNSs of individual third instar larvae were loaded one CNS per lane and blots were probed with an anti-synaptotagmin antibody [Dsyt-CL1 (Mackler et al., 2002)] and an anti-actin antibody (MAB 1501; Millipore Bioscience Research Reagents) using standard techniques (Loewen et al., 2001). Actin levels were used to normalize for equal protein loading; the synaptotagmin: actin signal ratio was determined for each lane, then normalized to the mean synaptotagmin:actin ratio of the $P[syt^{WT}]$ lanes on each blot to allow comparison of signal between multiple blots. Transgenic synaptotagmin was localized by immunolabeling third instar larvae with Dsyt-CL1 using standard techniques (Mackler and Reist, 2001). Neuromuscular junctions were visualized on a Zeiss Axioplan 2 upright digital imaging microscope.

Circular dichroism spectroscopy. Circular dichroism (CD) spectra were measured with an AVIV stop-flow circular dichroism spectropolarimeter at 192–260 nm using a 1 mm path-length cell. Samples containing 0.2 mg/ml of either wild-type or mutant C_2A domains were assayed at 22°C. For corrections of baseline noise, the signal from a blank run of buffer (50 mM sodium phosphate) was subtracted from all the experimental spectra.

Isothermal titration calorimetry. Isothermal titration calorimetry (ITC) data were generated using a GE Healthcare MicroCal iTC_{200}, which, in principle, can detect dissociation constants from 10 mM to 1 nM. Wild-type and mutant C_2A domains were dialyzed overnight in ITC buffer (50 mM HEPES, pH 7.4, 200 mM NaCl, and 10% glycerol). ITC buffer was further used to make calcium chloride stock and protein dilutions. Before each experiment, samples were degassed and cooled to experimental temperature. Heat of binding was measured from thirty 1.1 μl injections of calcium chloride into sample cells containing 1.6 mg/ml of proteins of interest at 15°C. Baseline corrections, for heat of dilution, were made by subtracting the signal of calcium chloride injections into buffer from all experimental traces. Data were analyzed using GE Healthcare MicroCal iTC_{200} Origin data software package.

Statistical analyses. A Student's *t* test was used to determine whether any statistically significant differences existed between the two independent $P[syt^{A\text{-}D2E}]$ lines (line 3 and line 5). One-way ANOVA and Tukey range tests were used for statistical comparisons of $P[syt^{WT}]$ and the two $P[syt^{A\text{-}D2E}]$ lines.

Results

Sequence and structural analyses of C_2A

C_2 domains are a common functional motif found in multiple proteins. Although not all C_2 domains are regulated by Ca^{2+}, many C_2 domains mediate a Ca^{2+}-dependent translocation of the protein to membranes (Nalefski and Falke, 1996; Cho and Stahelin, 2006). In these proteins, Ca^{2+} is coordinated by five negatively charged residues located in loops 1 and 3 of the C_2 domain β-sandwich structure (Fig. 1*A*,*B*, D1–D5) (Sutton et al., 1995; Nalefski and Falke, 1996; Ubach et al., 1998). Both aspartate and glutamate residues are used in the Ca^{2+}-binding motifs of diverse C_2 domains (Nalefski and Falke, 1996). To assess whether Ca^{2+} binding by C_2A could be supported by either aspartate or

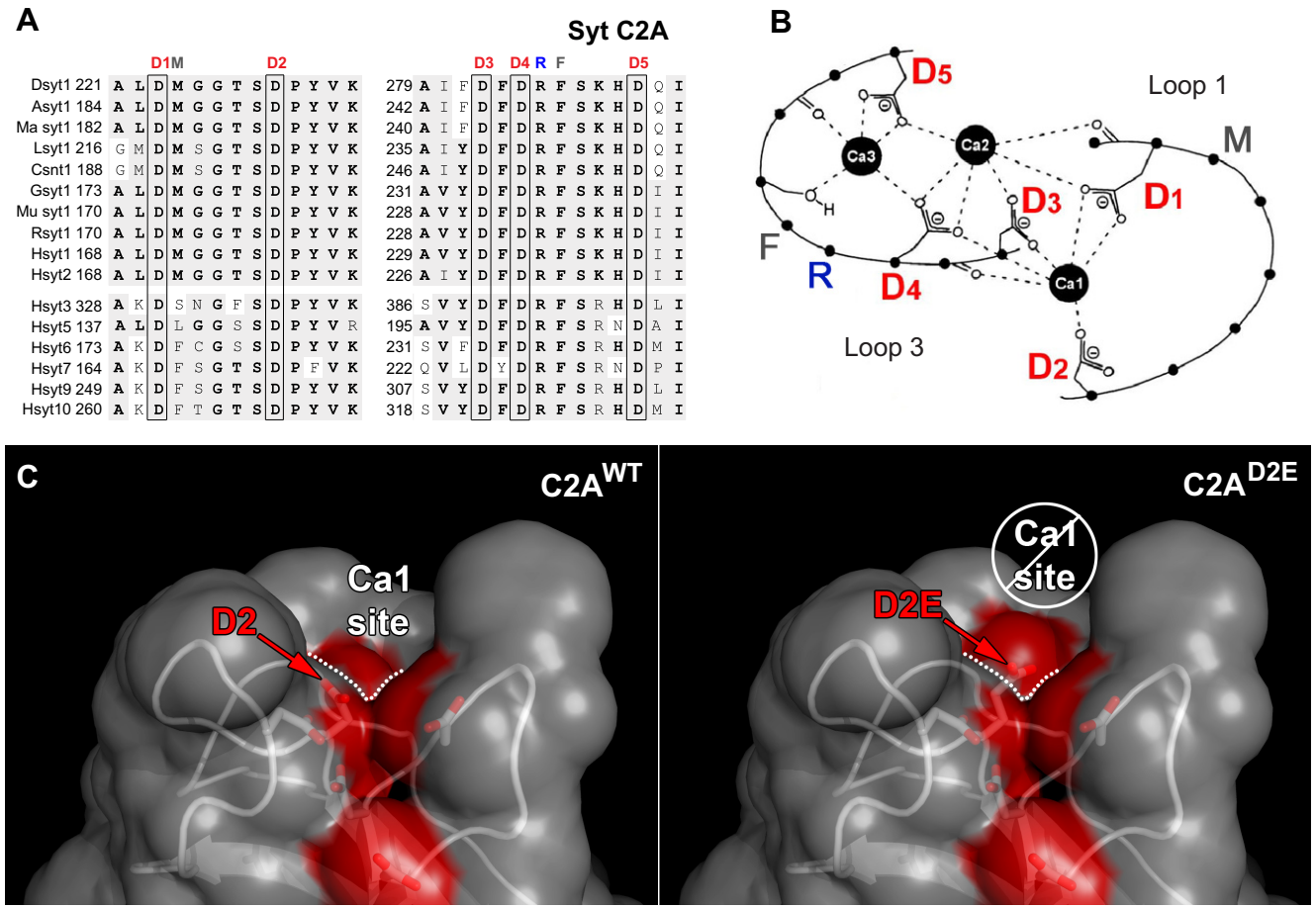

Figure 1. The C_2A domain of synaptotagmin 1 has five highly conserved aspartate residues that coordinate Ca^{2+}. ***A***, Alignment of C_2A from Ca^{2+}-binding synaptotagmin isoforms: synaptotagmin 1 from *Drosophila* (Dsyt1), bee (Asyt1), *Manduca* (Ma syt1), squid (Lsyt1), *C. elegans* (Csnt1), chicken (Gsyt1), mouse (Mu syt1), rat (Rsyt1), and human synaptotagmins (Hsyt) 1–3, 5–7, 9, and 10. Conserved residues are shown in gray and identical residues are in bold. The five conserved aspartate residues that coordinate the binding of Ca^{2+} ions are boxed and labeled as D1–D5. The conserved residues that mediate Ca^{2+}-dependent interactions with negatively charged membranes are also indicated by M, R, and F. ***B***, Schematic representation of loops 1 and 3 that form the Ca^{2+}-binding pocket of the C_2A domain. Adapted from Fernandez et al. (2001) to highlight the aspartates that coordinate Ca^{2+} (D1–D5) as well as the residues that interact with membranes (M, R, F). ***C***, Molecular model of the C_2A Ca^{2+}-binding pocket illustrating the potential effect of the C_2A^{D2E} mutation. Coloring the oxygen atoms of the aspartate residues that coordinate Ca^{2+} by element revealed the negatively charged Ca^{2+}-binding sites on the solvent accessible surface (red). In rat syt 1, asp178 (left, D2) participates in the coordination of the first Ca^{2+} (Ca1 site indicated by dotted line, see also ***B***). Using the mutagenesis function in PyMol, we modeled the consequences of altering asp178 to a glutamate (right, D2E). We predicted that the bulging out of the solvent accessible surface (right, enlarged red bulge above white dotted line) could prevent Ca^{2+} binding to the Ca1 site.

glutamate residues, we compared the sequence of C_2A domains of synaptotagmin isoforms that bind Ca^{2+}. A sequence alignment revealed that glutamate is excluded from these key positions. In the C_2A Ca^{2+}-binding motifs of synaptotagmin 1 from many species, as well as of all of the human synaptotagmin isoforms that bind Ca^{2+}, all five aspartate residues are 100% conserved (Fig. 1*A*), suggesting that glutamate residues in these positions would not provide full function.

Examination of the crystal structure of rat syt 1 C_2A demonstrates that the deepest parts of this Ca^{2+}-binding pocket are spatially quite restricted (Sutton et al., 1995). Glutamate, like aspartate, is negatively charged, but glutamate possesses a significantly larger molecular volume (91 $Å^3$ for Asp vs 109 $Å^3$ for Glu) (Creighton, 1994). Coupled with the exclusion of glutamate from C_2A Ca^{2+}-binding motifs, this observation suggests that a D⟶E mutation may impair Ca^{2+} binding. In the crystal structure of rat syt 1 C_2A, both aspartate residue 178 (Fig. 1*A*,*B*, D2) and aspartate residue 230 (Fig. 1*A*,*B*, D3) are well ordered and located deep in the Ca^{2+}-binding pocket (Sutton et al., 1995). To assess whether a D⟶E mutation in either of these locations may occlude the Ca^{2+}-binding pocket, we modeled the C_2A^{D2E} and C_2A^{D3E} mutations *in silico*. Results suggest that the C_2A^{D2E} mutation might occlude Ca^{2+}-binding site 1 (Fig. 1*C*, Ca1 site). If true, this novel mutation would directly assess the importance of the electrostatic repulsion provided by C_2A in inhibiting vesicle fusion since it would inhibit Ca^{2+} binding without reducing the negative charge of the pocket (Fig. 1*C*, red).

The syt$^{A\text{-}D2E}$ mutation inhibits Ca^{2+} binding to C_2A

To directly measure Ca^{2+} binding to the C_2A domain of *Drosophila* synaptotagmin 1, we used ITC. The titration data indicate three Ca^{2+}-binding sites in *Drosophila* C_2A (Fig. 2*A*, Table 1). The intrinsic Ca^{2+} affinities of the three sites measured by ITC (K_D values were: 20.7 ± 3.9 μM, 83.4 ± 19 μM, and 766 ± 302 μM, respectively; Table 1) were in the same range, though the K_Ds were somewhat lower than those in previous reports on murine synaptotagmin using NMR (Shao et al., 1996; Ubach et al., 1998). As predicted, Figure 2*A* demonstrates that the C_2A^{D2E} mutation inhibited Ca^{2+} binding by the C_2A domain. We assessed protein folding by CD spectroscopy to exclude misfolding of the mutant C_2A domain. As shown in Figure 2*B*, the C_2A^{D2E} mutation does not alter the CD spectrum compared with wild-type C_2A. Thus,

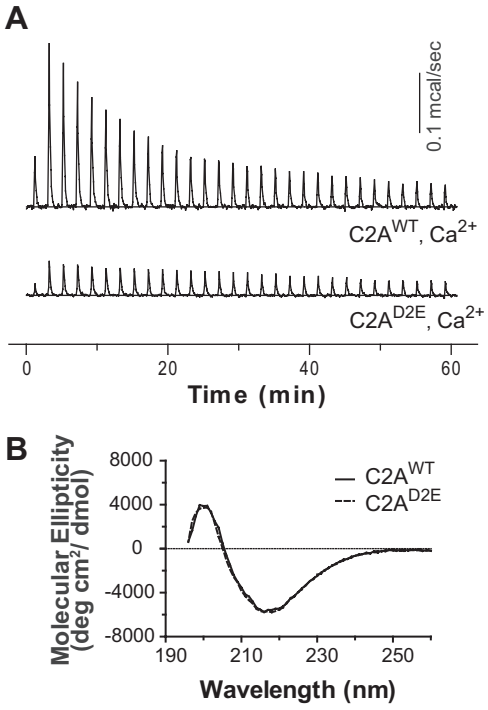

Figure 2. The C_2A^{D2E} mutation inhibits Ca^{2+} binding by C_2A without disrupting protein folding. ***A***, ITC analysis of Ca^{2+} binding to the isolated C_2A domain of WT and mutant *Drosophila* synaptotagmin 1; a representative Ca^{2+} titration is shown ($n = 3$). C_2A^{WT} bound three calcium ions (Table 1). The heat of binding of Ca^{2+} by C_2A^{D2E} was so small that the data could not be accurately fit. ***B***, C_2A^{D2E} is correctly folded. The CD spectra of the mutant domain (C_2A^{D2E}) was identical to wild-type (C_2A^{WT}).

Table 1. Thermodynamic properties of calcium binding to C_2A^{WT} using ITC

K_D (μM)	ΔH (cal/mol)	ΔS (cal/mol/K)	ΔG (kcal/mol)
$K_{D1} = 20.7 \pm 3.9$	$\Delta H_1 = 1005 \pm 72.3$	$\Delta S_1 = 24.9 \pm 0.12$	$\Delta G_1 = -6.17$
$K_{D2} = 83.4 \pm 19$	$\Delta H_2 = 407.5 \pm 166$	$\Delta S_2 = 20.1 \pm 0.35$	$\Delta G_2 = -5.38$
$K_{D3} = 766 \pm 302$	$\Delta H_3 = 2406 \pm 597$	$\Delta S_3 = 22.7 \pm 1.3$	$\Delta G_3 = -4.13$

Data represent mean $\pm$ SD, $n = 3$. K_D, Dissociation constant; Δ, change in; *H*, enthalpy; *S*, entrophy; *G*, Gibbs free energy.

our novel C_2A mutation is correctly folded and largely inhibits Ca^{2+} binding by the C_2A domain. D2 only directly coordinates the first Ca^{2+} site (Fig. 1*B*, D2–Ca1). If the C_2A^{D2E} mutation does in fact remove all Ca^{2+} binding, this would support a model in which Ca^{2+} binding to site 1 is requisite for Ca^{2+} binding to sites 2 and 3.

C_2A Ca^{2+}-binding mutant inhibits synchronous transmitter release *in vivo*

To determine the importance of electrostatic repulsion by the C_2A domain for synchronous synaptic transmission at an intact synapse, we examined evoked transmitter release at *Drosophila* neuromuscular junctions expressing our mutant transgenic synaptotagmin protein ($syt^{A\text{-}D2E}$) in the absence of any wild-type synaptotagmin 1. To indicate its transgenic origin, we will refer to the mutant as *P[syt$^{A\text{-}D2E}$]* and the transgenic controls as *P[syt^{WT}]*. We found that the $syt^{A\text{-}D2E}$ Ca^{2+}-binding motif mutation, which maintains the negative charge of the C_2A pocket, decreased synchronous evoked release by >80% (Fig. 3*A*,*B*). The amplitude of the EJP in *P[syt$^{A\text{-}D2E}$]* was 5.16 ± 0.96 mV (line 3, $n = 11$) or 2.84 ± 0.41 mV (line 2, $n = 8$) compared with 34.19 ± 3.97 ($n = 8$) in *P[syt^{WT}]* controls [Fig. 3*A* (line 3 shown), *B*, $p \ll 0.001$]. There was no significant difference between the independent mutant lines ($p > 0.07$), demonstrating that the decrease in evoked release is not due to the insertion sites of the transgene, but rather is a direct result of the mutation.

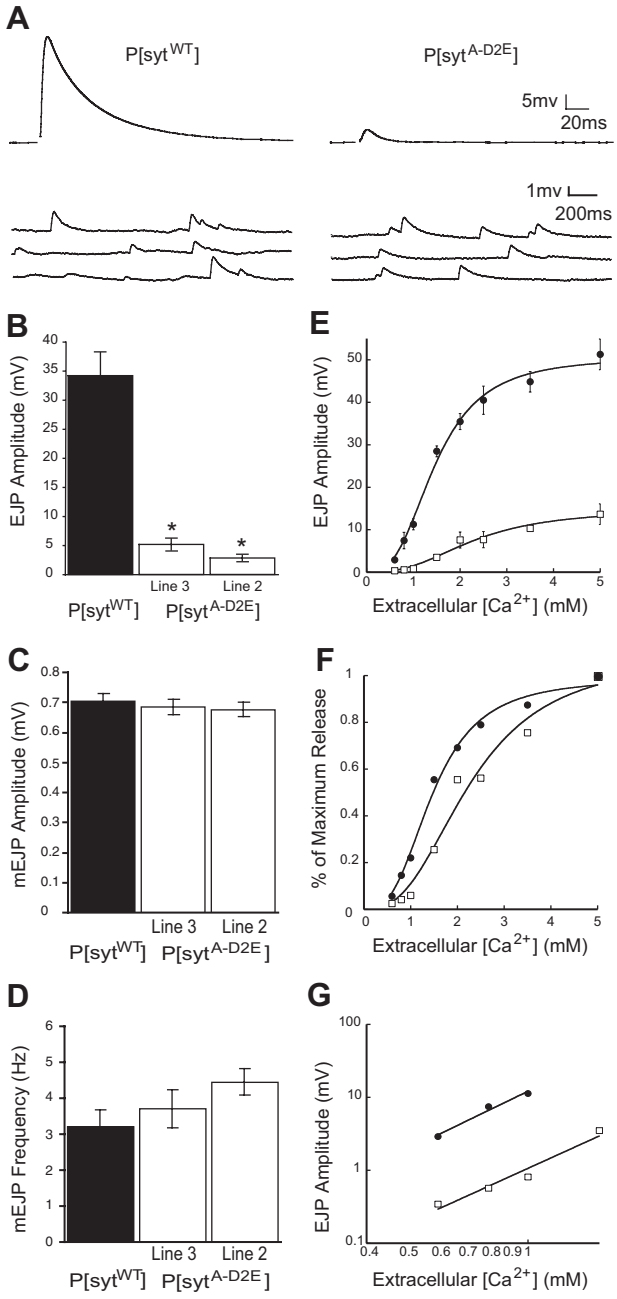

Figure 3. Synchronous evoked release is severely impaired in C_2A Ca^{2+}-binding mutants, but spontaneous release remains unchanged. ***A***, Representative traces of EJPs and mEJPs recorded in saline containing 1.5 mM [Ca^{2+}]. ***B***, Mean EJP amplitude was markedly decreased in *P[syt$^{A\text{-}D2E}$]* mutants compared with *P[syt^{WT}]* controls (mean $\pm$ SEM, $*p \ll 0.001$, one-way ANOVA). Neither mEJP amplitude (***C***, mean $\pm$ SEM, $p > 0.7$, one-way ANOVA) nor frequency (***D***, mean $\pm$ SEM, $p > 0.15$, one-way ANOVA) varied significantly between *P[syt$^{A\text{-}D2E}$]* mutants compared with *P[syt^{WT}]* controls. ***E***, EJP amplitude versus [Ca^{2+}] fit with the Hill equation. ***F***, Ca^{2+} dose–response data normalized to the maximal response in each line to illustrate the decrease in apparent Ca^{2+} affinity in the *P[syt$^{A\text{-}D2E}$]* mutant. ***G***, EJP amplitudes within the nonsaturating range of Ca^{2+} on a double log plot demonstrate that the Ca^{2+} cooperativity of release is not changed in the *P[syt$^{A\text{-}D2E}$]* mutants. A linear regression line was used to determine the slope. Error bars are SEM. Black circles indicate *P[syt^{WT}]*, white squares indicate *P[syt$^{A\text{-}D2E}$]*.

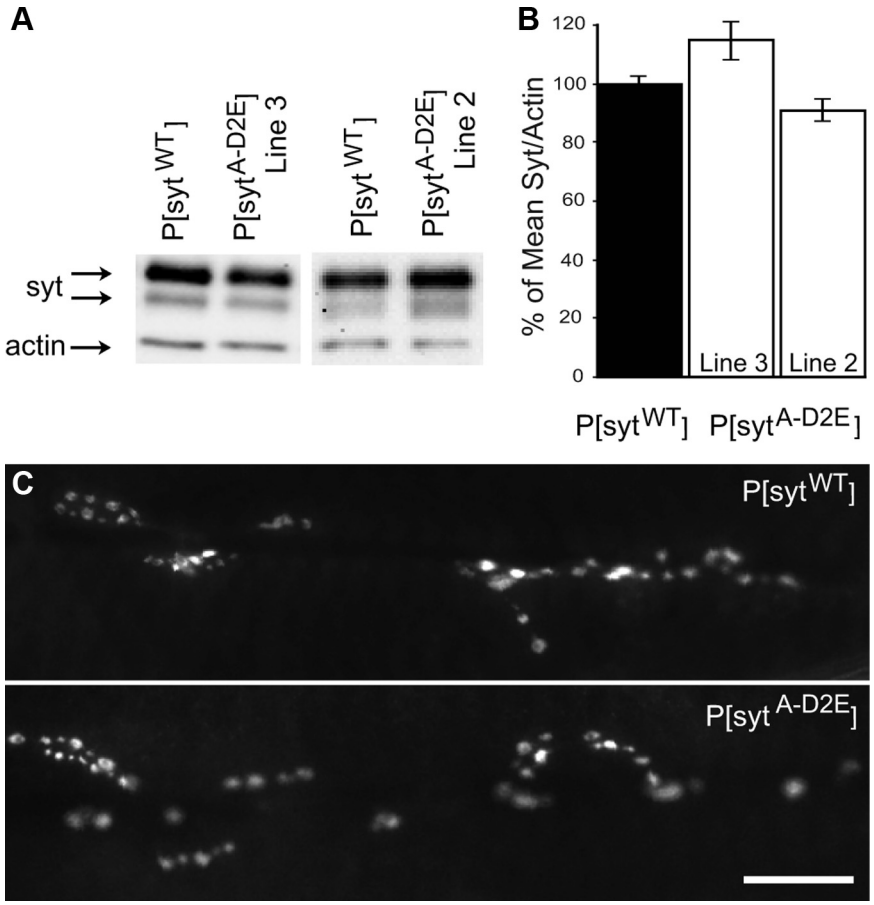

Figure 4. Synaptotagmin expression is similar in $P[syt^{A\text{-}D2E}]$ mutants compared with $P[syt^{WT}]$ controls. ***A***, Representative Western blots of the CNS of third instar larvae probed with anti-synaptotagmin and anti-actin antibodies. ***B***, Synaptotagmin:actin ratio normalized to the mean ratio of the transgenic control, $P[syt^{WT}]$. There was no significant difference between genotypes (mean ± SEM, $p > 0.3$, one-way ANOVA; $P[syt^{WT}]$, $n = 15$; $P[syt^{A\text{-}D2E}]$: line 3, $n = 6$; line 2, $n = 7$). ***C***, Synaptotagmin is properly localized to the larval neuromuscular junction in both mutant and control transgenic synaptotagmin lines. Scale bar, 20 μm.

Since analogous aspartate-to-asparagine mutations in C_2A, which also inhibit Ca^{2+} binding but partially neutralize the negative charge of the pocket, did not significantly impair synchronous evoked release at this same synapse (Robinson et al., 2002; Yoshihara et al., 2010) or at cultured excitatory synapses (Fernández-Chacón et al., 2002; Stevens and Sullivan, 2003), our findings demonstrate that the key function of Ca^{2+} binding to the C_2A domain is to neutralize the negative charge of the C_2A Ca^{2+}-binding pocket. Thus, Ca^{2+} binding to the C_2B domain is necessary and sufficient for synchronizing synaptic vesicle fusion to Ca^{2+} influx (Mackler et al., 2002; Robinson et al., 2002), as seen by the low level of fast, synchronous, evoked release that remains in our $P[syt^{A\text{-}D2E}]$ mutants (Fig. 3*A*,*B*). But it is not sufficient to efficiently trigger the electrostatic switch. Efficient, synchronous release requires Ca^{2+} binding to the C_2A and C_2B domains to neutralize both negatively charged Ca^{2+}-binding pockets and to flip the electrostatic switch resulting in fast, synchronous vesicle fusion.

C_2A mutant does not impact spontaneous transmitter release

The C_2A Ca^{2+}-binding motif mutation had no significant effect on either the amplitude or frequency of spontaneous transmitter release. The amplitude of mEJPs in $P[syt^{A\text{-}D2E}]$ was 0.69 ± 0.03 mV (line 3, $n = 12$) or 0.68 ± 0.03 mV (line 2, $n = 12$) compared with 0.70 ± 0.02 mV ($n = 12$) in $P[syt^{WT}]$ (Fig. 3*C*, $p > 0.7$). The constant mEJP amplitude demonstrates that synaptic vesicle filling and the postsynaptic response to neurotransmitter are unimpaired. The frequency of mEJPs in the C_2A mutants was also not significantly different at 3.71 ± 0.52 Hz (line 3) or 4.45 ± 0.37 Hz (line 2) in $P[syt^{A\text{-}D2E}]$ compared with 3.19 ± 0.48 Hz in $P[syt^{WT}]$ controls (Fig. 3*D*, $p > 0.15$). Since this C_2A Ca^{2+}-binding motif mutation results in a large decrease in evoked release (Fig. 3*A*,*B*), yet does not affect the rate of spontaneous release (Fig. 3*A*,*D*), the increase in spontaneous release seen in other synaptotagmin point mutants (Mackler and Reist, 2001; Mackler et al., 2002; Paddock et al., 2008) cannot be explained as an indirect developmental artifact resulting from the decrease in evoked release. Rather, our findings support the hypothesis that synaptotagmin plays a direct role in regulating the rate of spontaneous release (Broadie et al., 1994; Morimoto et al., 1995; Mace et al., 2009) and that the negative charge of the C_2A Ca^{2+}-binding pocket plays a key role in this process. Indeed, when Ca^{2+} binding is inhibited by D→N mutations of the C_2A Ca^{2+}-binding pocket, the rate of spontaneous release is increased sixfold (Yoshihara et al., 2010). This dramatic difference in the effect on spontaneous fusion frequency between D→N mutations and our D→E mutation demonstrates that the electrostatic repulsion created by the negative charge in the C_2A Ca^{2+}-binding pocket must be neutralized to enhance any fusion.

C_2A mutants decrease apparent Ca^{2+} affinity of release

To assess whether the decrease in evoked release resulted from changes in either the apparent Ca^{2+} affinity or cooperativity of release, we measured EJP amplitudes in extracellular Ca^{2+} concentrations ranging from 0.6 to 5 mM. $P[syt^{A\text{-}D2E}]$ had a significantly reduced evoked response compared with the control at every extracellular Ca^{2+} concentration (Fig. 3*E*). To facilitate comparison, the data were plotted as a percentage of the maximal response (Fig. 3*F*). The apparent Ca^{2+} affinity of release *in vivo* was decreased in the $P[syt^{A\text{-}D2E}]$ mutants; 45% more Ca^{2+} was required to trigger a half maximal response (EC_{50} = 1.92 ± 0.26 mM) compared with $P[syt^{WT}]$ controls (EC_{50} = 1.33 ± 0.18 mM). By plotting the mean EJP amplitude against the extracellular Ca^{2+} concentration at nonsaturating levels on a double log plot (Fig. 3*G*), we found that the Ca^{2+} cooperativity of release was not affected by the $syt^{A\text{-}D2E}$ mutation [$n = 2.52$ for $P[syt^{A\text{-}D2E}]$ and $n = 2.69$ for $P[syt^{WT}]$, similar to previously reported values at wild-type neuromuscular junctions in *Drosophila* (Stewart et al., 2000; Okamoto et al., 2005)]. The shift in the Ca^{2+} affinity of release with no effect on the cooperativity of release is consistent with the stochastic model of cooperativity (Dodge and Rahamimoff, 1967; Stewart et al., 2000; Fernández-Chacón et al., 2001; Mackler et al., 2002). However, some synaptotagmin mutations alter the cooperativity of release, which would favor the stoicheiometric model (Dodge and Rahamimoff, 1967; Yoshihara

and Littleton, 2002; Tamura et al., 2007). Further work will be necessary to discriminate between these models. Regardless, the decrease in the apparent Ca^{2+} affinity of evoked release is consistent with the finding that the $syt^{A\text{-}D2E}$ mutation specifically inhibits Ca^{2+} binding by the C_2A domain and demonstrates that Ca^{2+} binding by C_2A is essential for fast, synchronous synaptic transmission.

Transgene expression and distribution are unaffected

Since a decrease in synchronous evoked release could also result from protein misexpression, we assessed transgenic synaptotagmin expression levels in each transgenic line. Western blot analysis of third instar larval CNSs with an anti-synaptotagmin antibody demonstrated that the C_2A Ca^{2+}-binding motif mutant lines expressed similar levels of transgenic synaptotagmin as the transgenic control (Fig. 4*A*,*B*). In addition, the mutant synaptotagmin was appropriately localized to the neuromuscular junction (Fig. 4*C*). Therefore, the deficits in evoked release are not due to insufficient protein expression or protein mislocalization.

Discussion

Our results now clearly demonstrate that Ca^{2+} binding by the C_2A domain is a key functional component of the electrostatic switch that triggers synchronous synaptic vesicle fusion. A comparison of multiple C_2A Ca^{2+}-binding mutants reveals that the key function of Ca^{2+} binding by C_2A is to neutralize the negative charge of this pocket. Our D→E mutant inhibits Ca^{2+} binding but maintains the negative charge of the C_2A pocket. D→N mutants also inhibit Ca^{2+} binding, but they decrease the negative charge of the C_2A pocket. Neutralization of the C_2A pocket results in a dramatic increase in the fusion-stimulating activity of synaptotagmin.

Our C_2A D→E mutant inhibits Ca^{2+} binding but maintains the negative charge of the C_2A pocket. With the repulsive force of the C_2A domain intact, both synchronous release and the apparent Ca^{2+} affinity of release were decreased. In C_2A D→N mutants, synchronous transmitter release proceeds efficiently with Ca^{2+} binding to C_2B, providing the synchronization to Ca^{2+} influx (Fernández-Chacón et al., 2002; Robinson et al., 2002; Yoshihara et al., 2010). Indeed, C_2A D→N mutants that include D4N enhanced synchronous fusion as shown by an increase in the apparent Ca^{2+} affinity of release (Stevens and Sullivan, 2003; Pang et al., 2006; Yoshihara et al., 2010). The major difference between these mutants is the charge of the Ca^{2+}-binding pocket. Thus, the electrostatic repulsion provided by the C_2A domain must be neutralized, by either Ca^{2+} binding or mutation, to activate synaptotagmin's fusion-stimulating function during synchronous transmitter release. Interestingly, one multiple C_2A mutant ($C2A^{D2,3,4A}$) that both inhibits Ca^{2+} binding and neutralizes the negative charge of the pocket decreased synchronous release by ~30% at cultured inhibitory synapses (Shin et al., 2009). Yet similar multiple C_2A D→N mutations (even the $C2A^{D1\text{-}5N}$ mutation) do not decrease synchronous release (Stevens and Sullivan, 2003). The effect of these mutations on spontaneous release was not reported. This differential effect may indicate that neutral asparagine (vs alanine) residues more closely mimic Ca^{2+}-bound aspartates. Regardless of the source of these differences, the finding that our C_2A D→E mutation inhibits synchronous release by 80% demonstrates that the major mechanism used by C_2A to inhibit synaptotagmin's fusogenic activity is electrostatic repulsion.

The effect of mutations on spontaneous vesicle fusion events demonstrates that the negative charge of the C_2A pocket acts as a clamp to inhibit an inherent fusion-stimulating activity of synaptotagmin. Our C_2A D→E mutation maintains the ability of synaptotagmin to suppress spontaneous release, while C_2A D→N mutations result in a massive increase in spontaneous vesicle fusion events (Yoshihara et al., 2010). Thus, regardless of the downstream effector interaction(s) that mediate the fusion reaction, the negative charge of the C_2A Ca^{2+}-binding pocket functionally inhibits synaptic vesicle fusion until neutralized.

D→N mutations in both C_2A and C_2B increase the rate of spontaneous transmitter release (Mackler et al., 2002; Yoshihara et al., 2010), in effect removing the need for Ca^{2+} to unleash the fusion-stimulating activity of synaptotagmin. So why do these mutations impact synchronous release so differently? C_2B D→N mutants nearly completely block synchronous release (Mackler et al., 2002), while C_2A D→N mutants do not (Fernández-Chacón et al., 2002; Robinson et al., 2002; Yoshihara et al., 2010). Here we propose a possible mechanism (Fig. 5) that may contribute to this differential action, although additional interactions must also be involved, as noted below.

C_2B, by virtue of its Ca^{2+}-independent priming interaction with the SNARE complex (Rickman et al., 2004; Loewen et al., 2006b) and being the vesicle distal C_2 domain, would be located immediately adjacent to the presynaptic membrane, while C_2A is likely further removed. Before Ca^{2+} entry, electrostatic repulsion prevents interactions between the C_2 domains and the negatively charged presynaptic membrane (Fig. 5*A*,*B*, minus signs). Ca^{2+} influx initiates the electrostatic switch: an immediate change from electrostatic repulsion (due to the negatively charged residues) to electrostatic attraction of the negatively charged presynaptic membrane (due to the bound Ca^{2+} and the conserved, positively charged residue; Fig. 5*B*,*C*, blue sticks, plus signs), which pulls the vesicle toward the presynaptic membrane. Hydrophobic residues on the tip of the C_2 domain (Fig. 5*B*,*C*, gray sticks) can then penetrate the presynaptic membrane, destabilizing it and promoting the fusion reaction by pulling the presynaptic membrane toward the vesicle in a ring around the site of SNARE-mediated fusion (Fig. 5*D*). Since C_2B is located immediately adjacent to the presynaptic membrane, it would attract and penetrate the membrane first (Bai et al., 2002; Wang et al., 2003; Herrick et al., 2006; Fuson et al., 2007; Martens et al., 2007; Paddock et al., 2008, 2011; Hui et al., 2009). This action may then pivot the vesicle proximal C_2A domain toward the membrane where it can also then participate in the electrostatic attraction and hydrophobic penetration activities (Fernández-Chacón et al., 2001; Bai et al., 2002; Wang et al., 2003; Herrick et al., 2006; Paddock et al., 2008, 2011). When interactions of the C_2B domain with the presynaptic membrane are prevented by mutation, the C_2A domain would not be pivoted into position for interactions with the membrane and synaptic transmission would be blocked (Mackler et al., 2002; Paddock et al., 2011). When Ca^{2+} binding by the C_2A domain is inhibited via D→N mutations, the decreased negative charge of the pocket may partially mimic Ca^{2+} binding (Stevens and Sullivan, 2003), permitting the remaining C_2A lipid-interacting residues to bind and penetrate the presynaptic membrane when C_2B pivots the C_2A domain into position. Thus, these C_2A mutations would result in little to no disruption in evoked release (Fernández-Chacón et al., 2002; Robinson et al., 2002; Stevens and Sullivan, 2003; Pang et al., 2006). On the other hand, removal of the C_2A positively charged residue (Fig. 5*B*,*C*, C_2A, blue plus sign) or the hydrophobic residues (Fig. 5*B*,*C*, C_2A, gray sticks) by preventing C_2A from participating in effector interactions with the presynaptic membrane would result in a more

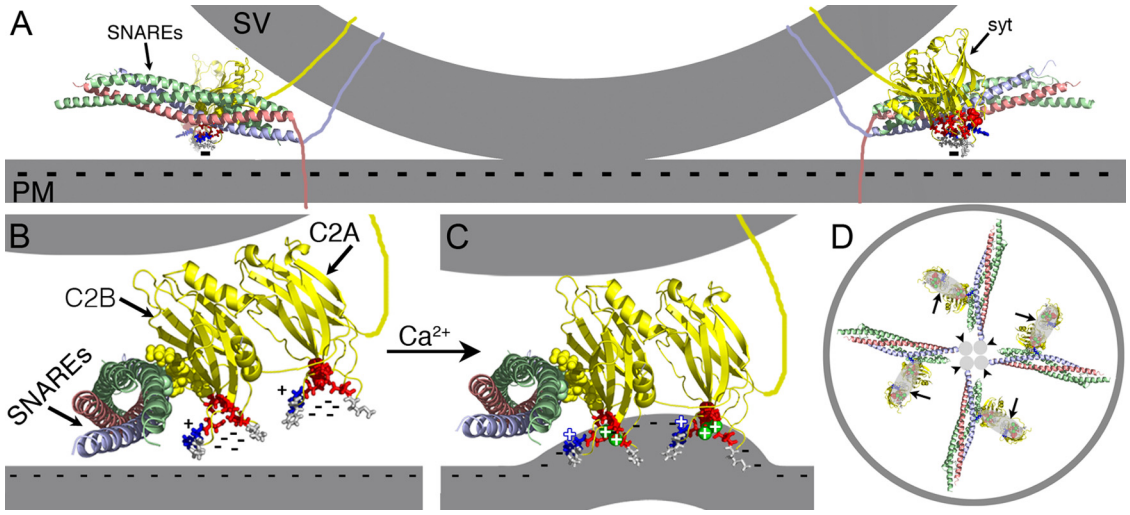

Figure 5. Ca^{2+} binding by C_2A is an essential component of the electrostatic switch. The crystal structure of the core complex [PDB file 1SFC, containing syntaxin (red), SNAP-25 (green), and VAMP/synaptobrevin (blue)], the NMR structures of the C_2A (PDB file 1BYN) and C_2B (PDB file 1K5W) domains of synaptotagmin (yellow), and Ca^{2+} (green circles with plus signs) are shown to scale using PyMOL. The membranes, the transmembrane domains, and the link between C_2A and C_2B were added in Adobe Photoshop. ***A***, Cross-section of a docked vesicle showing two SNARE complexes and their associated synaptotagmin molecules (syt). SC, Synaptic vesicle; PM, plasma membrane. ***B***, One synaptotagmin/SNARE complex viewed from the site of vesicle/presynaptic membrane apposition. A Ca^{2+}-independent docking/priming interaction between the C_2B polylysine motif (yellow, space-filled residues) and SNAP-25 (green, space-filled residues) (Rickman et al., 2004; Loewen et al., 2006b) holds the C_2B Ca^{2+}-binding site immediately adjacent to the presynaptic membrane with the C_2A Ca^{2+}-binding site further removed. In the absence of Ca^{2+}, the conserved aspartate residues (red residues: $syt^{C2A\text{-}D2}$, space-filled; the rest as sticks) within the pockets create a high concentration of negative charge (cluster of minus signs), resulting in electrostatic repulsion of the presynaptic membrane that prevents any membrane interactions by the tips of the C_2 domains. ***C***, Upon Ca^{2+} binding, the electrostatic repulsion of the pockets is neutralized, thereby initiating the electrostatic switch: a strong attraction of the negatively charged membrane by the bound Ca^{2+} (green circles with plus signs) and the basic residues at the tips of Ca^{2+}-binding pockets (blue stick residues, blue plus signs). Insertion of the hydrophobic residues (gray stick residues) at the tips of the C_2 domains into the core of the presynaptic membrane then triggers fusion by promoting a local Ca^{2+}-dependent positive curvature of the plasma membrane (Martens et al., 2007; Hui et al., 2009; Paddock et al., 2011). The C_2 domain interactions with the membrane likely pull the synaptic vesicle (upper gray membrane) toward the presynaptic membrane (lower gray membrane). The Ca^{2+}-induced increase in positive charge at the end of the C_2B domain also likely increases the strength of the electrostatic interaction between the C_2B polylysine motif and the SNARE complex, resulting in simultaneous binding of the SNARE complex and the presynaptic membrane (Davis et al., 1999; Bhalla et al., 2006; Loewen et al., 2006a; Dai et al., 2007). ***D***, Membrane penetration by multiple synaptotagmins (large gray ovals, arrows) would pull the plasma membrane toward the vesicle in a ring around the SNARE transmembrane domains (small gray circles, arrowheads) facilitating fusion.

severe disruption in evoked release (Fernández-Chacón et al., 2001; Paddock et al., 2008, 2011) than the D→N mutations.

Studies examining biochemical interactions between C_2A domains and negatively charged phospholipids *in vitro* may not fully reflect interactions *in vivo* due to the necessarily simplified environment of the *in vitro* assays. For instance, the positive charge of the Ca^{2+} bound to C_2A helps attract and bind negatively charged liposomes *in vitro*. D→N mutations in isolated C_2A domains inhibit this lipid binding despite charge neutralization (Fernández-Chacón et al., 2002; Robinson et al., 2002). But only one or two of the five negatively charged aspartates are mutated in the D→N mutations tested. Thus, this partial charge neutralization may be insufficient to actively attract negatively charged liposomes *in vitro*. Yet *in vivo*, active attraction by bound Ca^{2+} may not be necessary to permit near normal membrane interactions mediated by the remaining arginine and hydrophobic residues due to the coordinated action of the SNARE-associated C_2B domain to pivot the C_2A pocket onto the presynaptic membrane. Additional interactions not modeled above are undoubtedly also involved.

By inhibiting Ca^{2+} binding yet maintaining the negative charge of the pocket, the $syt^{A\text{-}D2E}$ mutation would interrupt all Ca^{2+}-dependent interactions mediated by C_2A; the effect would not be limited to the membrane interactions discussed in our model above. Indeed, since the $syt^{A\text{-}D2E}$ mutation results in an 80% decrease of synchronous release while the C_2A positively charged or hydrophobic mutations inhibit only 50% (Fernández-Chacón et al., 2001; Paddock et al., 2008, 2011), the impact of Ca^{2+} binding to C_2A clearly influences more than just these interactions with the membrane. Thus, C_2A likely participates in additional electrostatic interactions upon Ca^{2+} binding that play a role in triggering synchronous release, perhaps with SNARE complexes or other effector molecules. Regardless of which C_2A interactions trigger fusion, the finding that C_2A D→N mutations support efficient synaptic transmission while our C_2A D→E mutation inhibits transmission by 80% demonstrates the central importance of the change in electrostatic potential of C_2A for triggering fusion.

In summary, our current findings show severe disruption of synchronous synaptic transmission *in vivo* caused by inhibiting Ca^{2+}-binding by the C_2A domain without removal of the negative charge of the pocket. These results demonstrate that this negative charge in C_2A is a critical component of the electrostatic inhibition that prevents synaptic vesicle fusion. Thus, the essential function of Ca^{2+} binding to the C_2A domain of synaptotagmin is to neutralize this charge and, along with C_2B, to initiate the electrostatic switch mechanism that triggers vesicle fusion.

References

Bai J, Wang P, Chapman ER (2002) C2A activates a cryptic Ca^{2+}-triggered membrane penetration activity within the C2B domain of synaptotagmin I. Proc Natl Acad Sci U S A 99:1665–1670.

Bhalla A, Chicka MC, Tucker WC, Chapman ER (2006) Ca(2+)-synaptotagmin directly regulates t-SNARE function during reconstituted membrane fusion. Nat Struct Mol Biol 13:323–330.

Brand AH, Perrimon N (1993) Targeted gene expression as a means of altering cell fates and generating dominant phenotypes. Development 118:401–415.

Broadie K, Bellen HJ, DiAntonio A, Littleton JT, Schwarz TL (1994) Absence of synaptotagmin disrupts excitation-secretion coupling during synaptic transmission. Proc Natl Acad Sci U S A 91:10727–10731.

Brose N, Petrenko AG, Südhof TC, Jahn R (1992) Synaptotagmin: a calcium sensor on the synaptic vesicle surface. Science 256:1021–1025.

Chae YK, Abildgaard F, Chapman ER, Markley JL (1998) Lipid binding ridge on loops 2 and 3 of the C2A domain of synaptotagmin I as revealed by NMR spectroscopy. J Biol Chem 273:25659–25663.

Chapman ER, Davis AF (1998) Direct interaction of a Ca2+-binding loop of synaptotagmin with lipid bilayers. J Biol Chem 273:13995–14001.

Chapman ER, Hanson PI, An S, Jahn R (1995) Ca2+ regulates the interaction between synaptotagmin and syntaxin 1. J Biol Chem 270:23667–23671.

Cho W, Stahelin RV (2006) Membrane binding and subcellular targeting of C2 domains. Biochim Biophys Acta 1761:838–849.

Creighton TE (1994) Proteins: structure and molecular properties. New York: W. H. Freeman and Co.

Dai H, Shen N, Araç D, Rizo J (2007) A quaternary SNARE-synaptotagmin-Ca2+-phospholipid complex in neurotransmitter release. J Mol Biol 367:848–863.

Davis AF, Bai J, Fasshauer D, Wolowick MJ, Lewis JL, Chapman ER (1999) Kinetics of synaptotagmin responses to Ca2+ and assembly with the core SNARE complex onto membranes. Neuron 24:363–376.

Davletov B, Perisic O, Williams RL (1998) Calcium-dependent membrane penetration is a hallmark of the C2 domain of cytosolic phospholipase A2 whereas the C2A domain of synaptotagmin binds membranes electrostatically. J Biol Chem 273:19093–19096.

DiAntonio A, Parfitt KD, Schwarz TL (1993) Synaptic transmission persists in *synaptotagmin* mutants of *Drosophila*. Cell 73:1281–1290.

Dodge FA Jr, Rahamimoff R (1967) Co-operative action of calcium ions in transmitter release at the neuromuscular junction. J Physiol 193:419–432.

Elferink LA, Peterson MR, Scheller RH (1993) A role for synaptotagmin (p65) in regulated exocytosis. Cell 72:153–159.

Fernandez I, Araç D, Ubach J, Gerber SH, Shin O, Gao Y, Anderson RG, Südhof TC, Rizo J (2001) Three-dimensional structure of the synaptotagmin 1 C_2B-domain: synaptotagmin 1 as a phospholipid binding machine. Neuron 32:1057–1069.

Fernández-Chacón R, Königstorfer A, Gerber SH, García J, Matos MF, Stevens CF, Brose N, Rizo J, Rosenmund C, Südhof TC (2001) Synaptotagmin I functions as a calcium regulator of release probability. Nature 410:41–49.

Fernández-Chacón R, Shin OH, Königstorfer A, Matos MF, Meyer AC, Garcia J, Gerber SH, Rizo J, Südhof TC, Rosenmund C (2002) Structure/function analysis of Ca2+ binding to the C2A domain of synaptotagmin I. J Neurosci 22:8438–8446.

Fuson KL, Montes M, Robert JJ, Sutton RB (2007) Structure of human synaptotagmin 1 C2AB in the absence of Ca2+ reveals a novel domain association. Biochemistry 46:13041–13048.

Herrick DZ, Sterbling S, Rasch KA, Hinderliter A, Cafiso DS (2006) Position of synaptotagmin I at the membrane interface: cooperative interactions of tandem C2 domains. Biochemistry 45:9668–9674.

Hui E, Johnson CP, Yao J, Dunning FM, Chapman ER (2009) Synaptotagmin-mediated bending of the target membrane is a critical step in Ca(2+)-regulated fusion. Cell 138:709–721.

Loewen CA, Mackler JM, Reist NE (2001) *Drosophila synaptotagmin I* null mutants survive to early adulthood. Genesis 31:30–36.

Loewen CA, Royer SM, Reist NE (2006a) *Drosophila* synaptotagmin I null mutants show severe alterations in vesicle populations but calcium-binding motif mutants do not. J Comp Neurol 496:1–12.

Loewen CA, Lee SM, Shin YK, Reist NE (2006b) C2B polylysine motif of synaptotagmin facilitates a Ca2+-independent stage of synaptic vesicle priming in vivo. Molec Biol Cell 17:5211–5226.

Mace KE, Biela LM, Sares AG, Reist NE (2009) Synaptotagmin I stabilizes synaptic vesicles via its C2A polylysine motif. Genesis 47:337–345.

Mackler JM, Reist NE (2001) Mutations in the second C_2 domain of synaptotagmin disrupt synaptic transmission at *Drosophila* neuromuscular junctions. J Comp Neurol 436:4–16.

Mackler JM, Drummond JA, Loewen CA, Robinson IM, Reist NE (2002) The C(2)B Ca(2+)-binding motif of synaptotagmin is required for synaptic transmission in vivo. Nature 418:340–344.

Martens S, Kozlov MM, McMahon HT (2007) How synaptotagmin promotes membrane fusion. Science 316:1205–1208.

Morimoto T, Popov S, Buckley KM, Poo MM (1995) Calcium-dependent transmitter secretion from fibroblasts: modulation by synaptotagmin I. Neuron 15:689–696.

Murray D, Honig B (2002) Electrostatic control of the membrane targeting of C2 domains. Mol Cell 9:145–154.

Nalefski EA, Falke JJ (1996) The C2 domain calcium-binding motif: structural and functional diversity. Protein Sci 5:2375–2390.

Okamoto T, Tamura T, Suzuki K, Kidokoro Y (2005) External Ca2+ dependency of synaptic transmission in *drosophila* synaptotagmin I mutants. J Neurophysiol 94:1574–1586.

Paddock BE, Striegel AR, Hui E, Chapman ER, Reist NE (2008) Ca2+-dependent, phospholipid-binding residues of synaptotagmin are critical for excitation-secretion coupling in vivo. J Neurosci 28:7458–7466.

Paddock BE, Wang Z, Biela LM, Chen K, Getzy MD, Striegel A, Richmond JE, Chapman ER, Featherstone DE, Reist NE (2011) Membrane penetration by synaptotagmin is required for coupling calcium binding to vesicle fusion in vivo. J Neurosci 31:2248–2257.

Pang ZP, Shin OH, Meyer AC, Rosenmund C, Südhof TC (2006) A gain-of-function mutation in synaptotagmin-1 reveals a critical role of Ca2+-dependent soluble N-ethylmaleimide-sensitive factor attachment protein receptor complex binding in synaptic exocytosis. J Neurosci 26:12556–12565.

Reist NE, Buchanan J, Li J, DiAntonio A, Buxton EM, Schwarz TL (1998) Morphologically docked synaptic vesicles are reduced in *synaptotagmin* mutants of *Drosophila*. J Neurosci 18:7662–7673.

Rickman C, Archer DA, Meunier FA, Craxton M, Fukuda M, Burgoyne RD, Davletov B (2004) Synaptotagmin interaction with the syntaxin/SNAP-25 dimer is mediated by an evolutionarily conserved motif and is sensitive to inositol hexakisphosphate. J Biol Chem 279:12574–12579.

Robinson IM, Ranjan R, Schwarz TL (2002) Synaptotagmins I and IV promote transmitter release independently of Ca(2+) binding in the C(2)A domain. Nature 418:336–340.

Schiavo G, Stenbeck G, Rothman JE, Söllner TH (1997) Binding of the synaptic vesicle v-SNARE, synaptotagmin, to the plasma membrane t-SNARE, SNAP-25, can explain docked vesicles at neurotoxin-treated synapses [see comments]. Proc Natl Acad Sci U S A 94:997–1001.

Shao X, Davletov BA, Sutton RB, Südhof TC, Rizo J (1996) Bipartite Ca^{2+}-binding motif in C_2 domains of synaptotagmin and protein kinase C. Science 273:248–251.

Shin OH, Xu J, Rizo J, Südhof TC (2009) Differential but convergent functions of Ca2+ binding to synaptotagmin-1 C2 domains mediate neurotransmitter release. Proc Natl Acad Sci U S A 106:16469–16474.

Stevens CF, Sullivan JM (2003) The synaptotagmin C2A domain is part of the calcium sensor controlling fast synaptic transmission. Neuron 39:299–308.

Stewart BA, Mohtashami M, Trimble WS, Boulianne GL (2000) SNARE proteins contribute to calcium cooperativity of synaptic transmission. Proc Natl Acad Sci U S A 97:13955–13960.

Sutton RB, Davletov BA, Berghuis AM, Südhof TC, Sprang SR (1995) Structure of the first C2 domain of synaptotagmin I: a novel Ca2+/phospholipid-binding fold. Cell 80:929–938.

Tamura T, Hou J, Reist NE, Kidokoro Y (2007) Nerve-evoked synchronous release and high K+-induced quantal events are regulated separately by synaptotagmin I at *Drosophila* neuromuscular junctions. J Neurophysiol 97:540–549.

Ubach J, Zhang X, Shao X, Südhof TC, Rizo J (1998) Ca2+ binding to synaptotagmin: how many Ca2+ ions bind to the tip of a C2-domain? EMBO J 17:3921–3930.

Wang P, Wang CT, Bai J, Jackson MB, Chapman ER (2003) Mutations in the effector binding loops in the C2A and C2B domains of synaptotagmin I disrupt exocytosis in a nonadditive manner. J Biol Chem 278:47030–47037.

Yao KM, White K (1994) Neural specificity of elav expression: defining a *Drosophila* promoter for directing expression to the nervous system. J Neurochem 63:41–51.

Yoshihara M, Littleton JT (2002) Synaptotagmin I functions as a calcium sensor to synchronize neurotransmitter release. Neuron 36:897–908.

Yoshihara M, Guan Z, Littleton JT (2010) Differential regulation of synchronous versus asynchronous neurotransmitter release by the C2 domains of synaptotagmin 1. Proc Natl Acad Sci U S A 107:14869–14874.

Zhang X, Kim-Miller MJ, Fukuda M, Kowalchyk JA, Martin TF (2002) Ca2+-dependent synaptotagmin binding to SNAP-25 is essential for Ca2+-triggered exocytosis. Neuron 34:599–611.